

Lawrence Berkeley Laboratory, University of California, Berkeley, Calif. 94720.

¹J. D. Bjorken, Phys. Rev. **179**, 1547 (1969).

²Kinematic variables used here are squared four-momentum transfer, q^2 ; incident and scattered muon energy, E_0 and E' ; $\nu = E_0 - E'$; and $\omega = 2m\nu/q^2$.

³G. Miller *et al.*, Phys. Rev. D **5**, 528 (1972).

⁴R. P. Feynman, *Photon-Hadron Interactions* (Benjamin, New York, 1972).

⁵For example, radiative corrections do not scale exactly and the effect on the data/data ratio is of the order of 5%. The apparatus nonscaling correction on Λ^{-2} (defined in Table I) is estimated to be less than $20 \times 10^{-4} \text{ GeV}^{-2}$ by a Monte Carlo calculation.

⁶A. Bodek, Ph.D. thesis, Massachusetts Institute of Technology, 1973 (unpublished); A. Bodek *et al.*, Phys. Rev. Lett. **30**, 1087 (1973). The agreement between the Bodek fit to νW_2 and the SLAC-MIT D_2 data (assuming $R=0.18$) is better than 6% and typically better than 2% for ω' values above 9 at all q^2 values ($> 1 \text{ GeV}^2/c^2$) measured at SLAC. J. S. Poucher *et al.*, SLAC Report No. SLAC-PUB-1309, 1973 (unpublished), and (without tables of cross sections) Phys. Rev. Lett. **32**, 118 (1974). For large- ω events, use of ω' introduces insignificant

changes.

⁷Variation of $R (= \sigma_s/\sigma_t)$ between 0 and ∞ could give rise to changes of order 10% in the ratios in Fig. 2.

⁸The Fermi motion correction is a function of ω only. See G. B. West, Ann. Phys. (New York) **14**, 464 (1972).

⁹K. W. Chen, Bull. Amer. Phys. Soc. **19**, 100 (1974). The preliminary results reported correspond to Fig. 2(g).

¹⁰This agreement checks the Monte Carlo assumptions since these data are even more sensitive to the variation of acceptance in q^2 and ω than data outside the SLAC kinematic region. The enhancement of $\omega > 9$ events remains as the acceptance is varied from 12% to over 65% (by varying q^2).

¹¹A. Entenberg *et al.*, Phys. Rev. Lett. **32**, 486 (1974); J. Kim *et al.*, to be published.

¹²The 150/56.3 ratio is "constrained" to 1.0 ± 0.05 . The data-to-Monte Carlo ratios are constrained to $N = 0.925 \pm 0.038$ (Ref. 11) times an estimated detection efficiency of 0.95 ± 0.10 .

¹³The acceptance is primarily defined by the maximum and minimum scattering angle and this is a function of q^2 and ω . Figure 2(e) shows the average acceptance versus q^2 .

Effect of $N^*(1236)$ on Radiative Muon Capture in Calcium

Kohichi Ohta

Institute of Physics, University of Tokyo, Komaba, Meguro-ku, Tokyo 153, Japan

(Received 19 September 1974)

Influence of the one-pion exchange current brought about by the $N^*(1236)$ excitation is considered for the photon spectrum of radiative muon capture in calcium. It is found that the relative rate of radiative to ordinary muon capture is substantially lowered and that the discrepancy between partial conservation of axial-vector current theory and experiment is removed.

A recent experiment¹ which measured the energy spectrum of the internal bremsstrahlung of radiative muon capture in calcium presents a puzzling problem. The experimental spectrum is completely inconsistent with a shell-model calculation based on the effective Hamiltonian for radiative muon capture by a free proton.² In the effective Hamiltonian the Goldberger-Treiman prediction³ is used to express the induced pseudoscalar form factor h_A in terms of the axial-vector form factor $g_A \cong 1.24$. However because of the nonconservation of the axial current, the effective g_A and h_A to be used for a nucleon bound in a nucleus cannot be the same as those for a free nucleon. Indeed it was found that in ordinary muon capture both g_A and h_A are reduced as a result of exchange current arising from the $N^*(1236)$ isobar.⁴

In this note I show that inclusion of the hitherto neglected effect of the pion exchange current removes the necessity for unfounded alteration of h_A from the partial conservation of axial-vector current (PCAC) prediction.

The matrix element for the process in which a stopped muon is absorbed while a γ ray is given off by two nucleons interacting through the exchange of a pion is obtained by inserting a photon at all possible places in the corresponding nonradiative Feynman diagram. The resulting set of diagrams is

shown in Fig. 1. The matrix element is decomposed into three parts, $T = T^{(1)} + T^{(2)} + T^{(3)}$, where

$$T^{(1)} = -(g/\sqrt{2}) \langle \pi^n(Q) N(p_1') | J_\alpha^A | N(p_1) \rangle (Q^2 + m_\pi^2)^{-1} \langle N(p_2') | J_\pi^n | N(p_2) \rangle \times \bar{u}(\nu) \gamma_\alpha (1 + \gamma_5) [i \gamma \cdot (\mu - k) + m_\mu]^{-1} i e \gamma \cdot \epsilon^{(\lambda)} u(\mu) + (1 \leftrightarrow 2), \quad (1)$$

$$T^{(2)} = (g/\sqrt{2}) \langle \pi^n(Q) N(p_1') | J_\alpha^A | N(p_1) \rangle (Q^2 + m_\pi^2)^{-1} \langle \gamma(k) N(p_2') | J_\pi^n | N(p_2) \rangle \times \bar{u}(\nu) \gamma_\alpha (1 + \gamma_5) u(\mu) + (1 \leftrightarrow 2), \quad (2)$$

$$T^{(3)} = (g/\sqrt{2}) \langle \pi^n(Q) \gamma(k) N(p_1') | J_\alpha^A | N(p_1) \rangle (Q^2 + m_\pi^2)^{-1} \langle N(p_2') | J_\pi^n | N(p_2) \rangle \times \bar{u}(\nu) \gamma_\alpha (1 + \gamma_5) u(\mu) + (1 \leftrightarrow 2). \quad (3)$$

Here g is the Fermi constant, $e^2/4\pi = 1/137$, m_π is the pion mass, and m_μ is the muon mass. The four-momentum of each particle is indicated in parentheses. Note that the momentum transfer at the vertex for weak interaction is $q = \mu - \nu$ in $T^{(2)}$ and $T^{(3)}$ while it becomes $s = q - k$ in $T^{(1)}$ corresponding to Fig. 1(a). The superscript n refers to the isotopic index of the pion and $\epsilon^{(\lambda)}$ to the polarization of the emitted photon, with λ indicating the sign of circular polarization. Conservation of vector current assures us that the vector-current form factors are unaffected by the interaction currents at zero momentum transfer. Moreover they have a much weaker dependence on q^2 than that of h_A so that we consider only the processes mediated by the axial current J_α^A .

In these processes the axial current can produce the intermediate $N^*(1236)$ isobar which we shall treat as an elementary particle in the Rarita-Schwinger scheme.⁵ The matrix element for N^* production by the axial current is written as

$$\langle N^*(p^*) | J_\alpha^A | N(p) \rangle = \bar{u}_\beta(p^*) (b_1 \delta_{\beta\alpha} + b_4 q_\beta q_\alpha) u(p). \quad (4)$$

The b_2 and b_3 terms are neglected for their smallness. Berman and Veltman⁶ show that the PCAC hypothesis and the pion-pole dominance of b_4 give $b_1 = -(G/m_\pi) f_\pi$ and $b_4 = -b_1/(q^2 + m_\pi^2)$, where $G^2/4\pi \cong 0.137$ and $f_\pi \cong 0.97 m_\pi$. As for the propagator of N^* we make use of the form $(\delta_{\alpha\beta} - \frac{1}{3} \gamma_\alpha \gamma_\beta) / (i \gamma \cdot p^* + M_{N^*})$, dropping terms of order p^*/M_{N^*} ($M_{N^*} = 1236$ MeV).

The weak pion production amplitude $\langle \pi N | J_\alpha^A | N \rangle$ in nuclear medium can be calculated by analogy to the model of Barshay, Brown, and Rho⁷ for pion scattering, if we substitute the weak vertex, Eq. (4), for one πNN^* vertex in their model [see also Chemtob and Rho⁸].

The amplitude for radiative pion absorption, $\langle \gamma N | J_\pi^n | N \rangle$, is given as the matrix element of the axial current by using both gauge invariance and PCAC.⁹ The amplitude consists of the seagull diagram, Fig. 1(b), the nucleon-pole diagrams, Figs. 1(c) and 1(d), and the pion-pole diagram, Fig. 1(e).

The transition amplitude for weak pion production accompanying bremsstrahlung, $\langle \pi \gamma N | J_\alpha^A | N \rangle$, is related to the radiative πN scattering.¹⁰ Correspondingly the pion-pole diagram, Fig. 1(f), and the contact terms represented by Figs. 1(g)–1(i) form an essential part. We omit smaller contributions from the nucleon bremsstrahlung diagrams, Figs. 1(j) and 1(k), and the photon radiation from the isobar corresponding to Fig. 1(l).

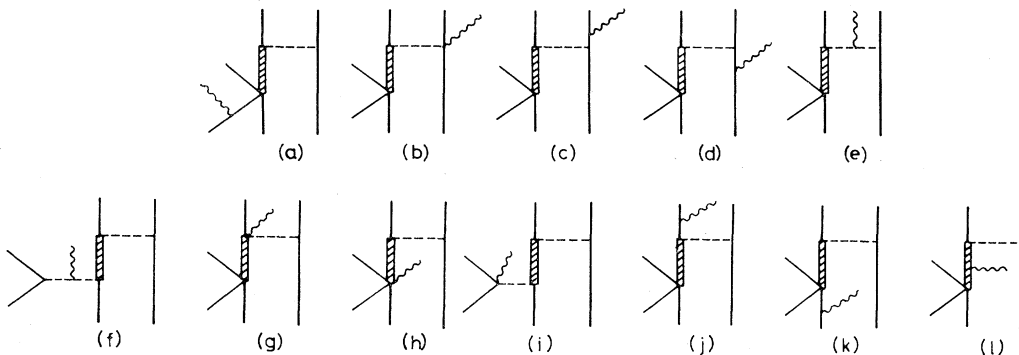


FIG. 1. Diagrams contributing to radiative muon capture by a two-nucleon system. The dashed line represents a pion and the wavy line a photon. The intermediate rectangle is N or N^* .

For the πNN vertex we use the usual form $\langle N(p_2') | J_\pi^a | N(p_2) \rangle = i(g_r/2M_N)\tau^a \vec{\sigma} \cdot \vec{Q}$, with g_r being the πN coupling constant and M_N the nucleon mass. In what follows we eliminate g_r by using the celebrated relation $f_\pi g_r = \sqrt{2}M_N g_A$ and rewrite the final result by means of g_A .

The effective two-body Hamiltonian responsible for radiative muon capture is given by transforming the matrix element T into configuration space following the standard prescription.⁸ To give an insight into the contribution from the interaction current let us express the effect of the two-body operator in terms of an effective one-body operator associated to a spectator nucleon by calculating contributions from the diagrams involving nucleon-hole and isobar-hole bubbles. In order to describe a strong repulsion at small NN distance, we employ a pair correlation function given by Day.¹¹

For a system of equal numbers of neutrons and protons, the nucleon-hole excitation does not contribute to the transition matrix element in the static limit. We are left with only the terms from the intermediate isobar so that the matrix element T gives an effective correction to the single-nucleon matrix element,

$$\delta T = \alpha (\frac{1}{2}\sqrt{2}g_A) e \vec{\epsilon}^{(\lambda)} \cdot (\vec{M}^{(1)} + \vec{M}^{(2)} + \vec{M}^{(3)}) \tau^- . \quad (5)$$

Here the coherent optical parameter $\alpha = -4\pi\rho c_0$ enters, where ρ is the nuclear density, $4\pi c_0 = 8G^2/3\omega^* m_\pi^2$, and $\omega^* = M_{N^*} - M_N$.¹² The energy of the pion relevant for the processes in Fig. 1 is $q_0 = m_\mu - \nu$ or $s_0 = m_\mu - \nu - k \cong 0$ so that the relative variation of c_0 with pion energy cannot exceed $(m_\mu/\omega^*)^2 \cong 0.1$, which enables us to neglect the energy dependence of c_0 .

We can now state the results for $\vec{M}^{(1)}$, $\vec{M}^{(2)}$, and $\vec{M}^{(3)}$:

$$\vec{M}^{(1)} = -(\lambda_+/m_\mu) \vec{\sigma} \cdot \vec{T}(s) \vec{\sigma}_i , \quad (6)$$

$$\vec{M}^{(2)} = \frac{q \cdot L(q)}{q^2 + m_\pi^2} \left[\left(1 + \frac{q_0}{2M_N} \right) \vec{\sigma} - \frac{2}{s^2 + m_\pi^2} \vec{q} \vec{\sigma} \cdot \vec{s} \right] + \frac{\lambda}{2M_N} [\mu^\nu \vec{T}(q) + \vec{\sigma} \cdot \vec{T}(q) \vec{\sigma}] , \quad (7)$$

$$\vec{M}^{(3)} = [\vec{\sigma} \cdot \vec{s} / (s^2 + m_\pi^2)] \{ \vec{L}(q) - 2[s^2 / (s^2 + m_\pi^2)] - \frac{1}{3} \xi_0 \} \vec{L}_p(q) + \vec{M}^{(3)'} , \quad (8)$$

and $\vec{\epsilon}^{(\lambda)} \cdot \vec{M}^{(3)'} = \vec{\sigma} \cdot \vec{T}'(s)$. Here $\lambda_+ = (1 + \lambda)/2$, $\mu^\nu = 3.7$, and $\vec{\sigma}_i$ refers to the spin operator of the lepton. The further notation is

$$\vec{T}(q) = [q \cdot L(q) / (q^2 + m_\pi^2)] \vec{q} - \frac{1}{3} \xi_0 \vec{L}(q) , \quad (9)$$

where $L_\alpha(q) = \bar{u}(\nu) [\gamma_\alpha - q_\alpha q \cdot \gamma / (q^2 + m_\pi^2)] (1 + \gamma_5) u(\mu)$; $\vec{L}_p(q)$ is the pion-pole part of $\vec{L}(q)$; $\vec{T}'(s)$ follows from $\vec{T}(s)$ by the minimal substitution for $\vec{L}(s)$; ξ_0 is the factor appearing in the π -nucleus optical potential.¹³

The final result is written down as corrections to the ten amplitudes g_1, \dots, g_{10} defined in terms of the spin combinations introduced by Rood and Tolhoek.¹⁴ By repeated use of the relations $h_A^L = 2M_N g_A / (s^2 + m_\pi^2)$ and $h_A^N = 2M_N g_A / (q^2 + m_\pi^2)$ the effect of these correction terms can be simply described by renormalizing the axial-current form factors according to the formulas

$$\tilde{g}_A = g_A (1 + \frac{1}{3} \xi_0 \alpha) , \quad (10)$$

$$\tilde{h}_A^L = h_A^L \left(1 - \frac{\delta m_\pi^2(s^2)}{s^2 + m_\pi^2} \right) + \alpha h_A^L , \quad (11)$$

$$\tilde{h}_A^N = h_A^N \left(1 - \frac{\delta m_\pi^2(q^2)}{q^2 + m_\pi^2} \right) + \alpha h_A^N , \quad (12)$$

in g_1, \dots, g_4, g_6 , and g_7 . Here $\delta m_\pi^2(q^2) = \alpha [q^2 - \frac{1}{3} \xi_0 (q^2 + m_\pi^2)]$. The g_5 and $g_8 = -g_9$ are unmodi-

fied. The amplitude g_{10} becomes

$$\tilde{g}_{10} = g_{10} \left(1 - \frac{\delta m_\pi^2(s^2)}{s^2 + m_\pi^2} + \alpha - \frac{\delta m_\pi^2(q^2)}{q^2 + m_\pi^2} + \alpha \right) . \quad (13)$$

The quenching of g_A , Eq. (10), is referred to as the Lorentz-Lorenz effect.¹⁵

With the modified one-body Hamiltonian, we can calculate the energy spectrum of the photons with the aid of the model of Rood and Tolhoek² who assume an independent-particle model for ^{40}Ca and apply the closure approximation to a shell model with harmonic-oscillator wave functions.¹⁶ The model obliges us to introduce two parameters: k_m , the maximum photon energy for an average excitation of the nucleus, and ν_{av} , the average neutrino energy in the ordinary capture. We cannot avoid theoretical uncertainties in determining the values of these parameters. To illustrate the main feature of the present model we fix $k_m = 89.4$ MeV and $\nu_{av} = 90.4$ MeV as used in Ref. 1. The suppression factor of the Lorentz-Lorenz effect, ξ_0 , is estimated to be 0.31 when the πN vertex function of Dürr and Pilkuhn¹⁷ is used.¹⁸

In order to compare with experiment we fold the resolution function obtained in Ref. 1 into the

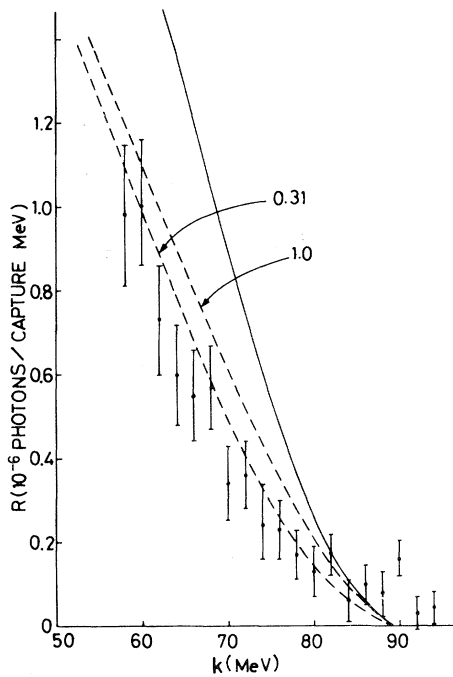


FIG. 2. Relative rate of radiative to normal muon capture. The solid line represents the relative rate predicted by Rood and Tolhoek while the broken lines show the result of the present calculations for indicated values of ξ_0 . The experimental data are taken from Ref. 1.

theoretical photon spectrum. Figure 2 shows the calculated spectrum $R(k)$ as a function of the photon energy k . For comparison the result for $\xi_0 = 1$ (the full Lorentz-Lorenz effect) is also presented.

From this figure it is observed that the exchange current is effective in reducing $R(k)$ and that the discrepancy between the PCAC prediction and experiment is significantly improved. The effect of the quenching of g_A on the ratio of radiative to normal capture is negligible although it is instrumental in lowering both of these rates

separately. The decrease of $R(k)$ is chiefly brought about by the term αh_A^N in Eq. (12) which is greatly enhanced at the high-energy end of the radiative spectrum ($q^2 \cong -m_\mu^2$) compared with the value for ordinary capture ($q^2 \cong m_\mu^2$).

In conclusion in view of both theoretical and experimental uncertainties it does not appear that the PCAC theory conflicts with experiment.

¹L. M. Rosenstein and I. S. Hammerman, Phys. Rev. C **8**, 603 (1973).

²H. P. C. Rood and H. A. Tolhoek, Nucl. Phys. **70**, 658 (1965).

³M. L. Goldberger and S. B. Treiman, Phys. Rev. **111**, 354 (1958).

⁴K. Ohta and M. Wakamatsu, Phys. Lett. **51B**, 325, 337 (1974), and to be published.

⁵W. Rarita and J. Schwinger, Phys. Rev. **60**, 61 (1941).

⁶S. M. Berman and M. Veltman, Nuovo Cimento **38**, 993 (1965).

⁷S. Barshay, G. E. Brown, and M. Rho, Phys. Rev. Lett. **32**, 787 (1974).

⁸M. Chemtob and M. Rho, Nucl. Phys. **A163**, 1 (1971).

⁹G. W. Gaffney, Phys. Rev. **161**, 1599 (1967).

¹⁰R. E. Cutkosky, Phys. Rev. **109**, 209 (1958).

¹¹B. Day, Phys. Rev. **187**, 1269 (1969).

¹²M. Rho, to be published.

¹³J. M. Eisenberg, J. Hüfner, and E. J. Moniz, Phys. Lett. **47B**, 381 (1973).

¹⁴See Eqs. (2.13) and (2.15) of Ref. 2. For g_A , g_P , and \tilde{g} of Ref. 2, read $-(g/\sqrt{2})g_A$, $-(g/\sqrt{2})m_\mu h_A$, and $-\tilde{g}$, respectively.

¹⁵M. Ericson, A. Figureau, and C. Thévenet, Phys. Lett. **45B**, 19 (1973). See also Refs. 12 and 4.

¹⁶The effect of NN forces greatly reduces both radiative and normal capture rates but their ratio is almost independent of residual interactions. E. Borchini and S. De Gennaro, Phys. Rev. C **2**, 1012 (1970).

¹⁷H. P. Dürr and H. Pilkuhn, Nuovo Cimento **40**, 899 (1965).

¹⁸The same correlation function and vertex function are used by B. H. J. McKellar and R. Rajaraman, Phys. Rev. Lett. **31**, 1063 (1973).